APPLIED ORGANOMETALLIC CHEMISTRY
Appl. Organometal. Chem. 2003; **17**: 480–492
Published online in Wiley InterScience (www.interscience.wiley.com). DOI:10.1002/aoc.462

Condensed polyhedral boranes and analogous organometallic clusters: a molecular orbital and density functional theory study on the cap–cap interactions†

Eluvathingal D. Jemmis* and Pattath D. Pancharatna

School of Chemistry, University of Hyderabad, Hyderabad 500 046, India

Received 7 January 2003; Revised 3 February 2003; Accepted 18 February 2003

The interactions between the non-bonded atoms on adjacent units were assumed to be one of the major factors that hinder the exploration and advancement of macropolyhedral borane chemistry. In sandwich complexes involving boron as the bridging atom, the interaction between non-bonded atoms tends to be antibonding, but a closer analysis of various condensed systems shows that this cannot be generalized. The overlap populations (OPs) calculated for structures optimized at the B3LYP/6-31g* level [$B_{21}H_{18}^{1-}$ (5), $B_{20}H_{16}$ (6), $[Al(C_2B_4H_6)_2]^{1-}$ (7), $B_{12}H_{10}^{2-}$ (8), $B_{10}H_8^{2-}$ (9 and 14), $B_{11}H_{13}$ (10), $B_{10}H_{14}$ (11), $C_2B_8H_{12}$ (13) and $B_{20}H_{18}^{2-}$ (15)] indicate bonding interactions between the caps, except for 7 and 13. This is substantiated by a detailed extended Hückel-based molecular orbital (MO) study using $B_{10}H_{14}$ as a model system to represent macropolyhedral boranes with higher fusions. An isolobal equivalent structure, $[C_8H_6(Ru(CO)_2Me)_2]$ (17), studied at the B3LYP/LANL2DZ level has weak Ru–Ru interactions. An analysis of the nature of the MOs in $B_{10}H_{14}$ (11) shows that there is no direct head on overlap of the cap orbitals that are antibonding; this is in contradiction to sandwiched molecules (7), where there are two occupied MOs with antibonding interactions. The $m + n + o$ electron pair count (m is the number of cages involved in condensation, n is the number of vertices and o is the number of single vertex condensations) of sandwich complexes requires the filling of these two MOs. The negative OP between the carbon atoms in 13 is attributed to the greater electronegativity of carbon and is substantiated by a fragment MO analysis. Copyright © 2003 John Wiley & Sons, Ltd.

KEYWORDS: macropolyhedral boranes; organometallic clusters; *ab initio*; molecular orbital calculations; DFT; *mno* rule

INTRODUCTION

The development of polyhedral borane chemistry has often involved isoelectronic and isolobal relationships with carbon and metals connecting boranes to hydrocarbons and to organometallics.[1,2] Various attempts to merge organometallics with boranes are carried out mostly through the intermediacy of metallaboranes and metallocenes.[3–5] Here, we use the examples known in organometallic chemistry to gain a better understanding of bonding in isolobally related and structurally similar polyhedral boranes. The major focus is on the interactions between two subclusters in a fused system. Steric interactions induced between two adjacent vertices of an icosahedron by replacing terminal hydrogen atoms with bulky substituents have been studied previously; a representative example is shown by **1** (Fig. 1).[6] In these molecules, mostly metallacarboranes, the phenyl groups on two neighboring carbon atoms result in repulsive interactions, leading to the cleavage of the C–C bond. The ligands on the metal are mostly Cp or C_6H_6, which

*Correspondence to: Eluvathingal D. Jemmis, School of Chemistry, University of Hyderabad, Hyderabad 500 046, India.
E-mail: jemmis@uohyd.ernet.in
†Dedicated to Professor Thomas P. Fehlner on the occasion of his 65th birthday, in recognition of his outstanding contributions to organometallic and inorganic chemistry.
Contract/grant sponsor: Council of Scientific and Industrial Research, New Delhi.
Contract/grant sponsor: Board of Research in Nuclear Sciences.

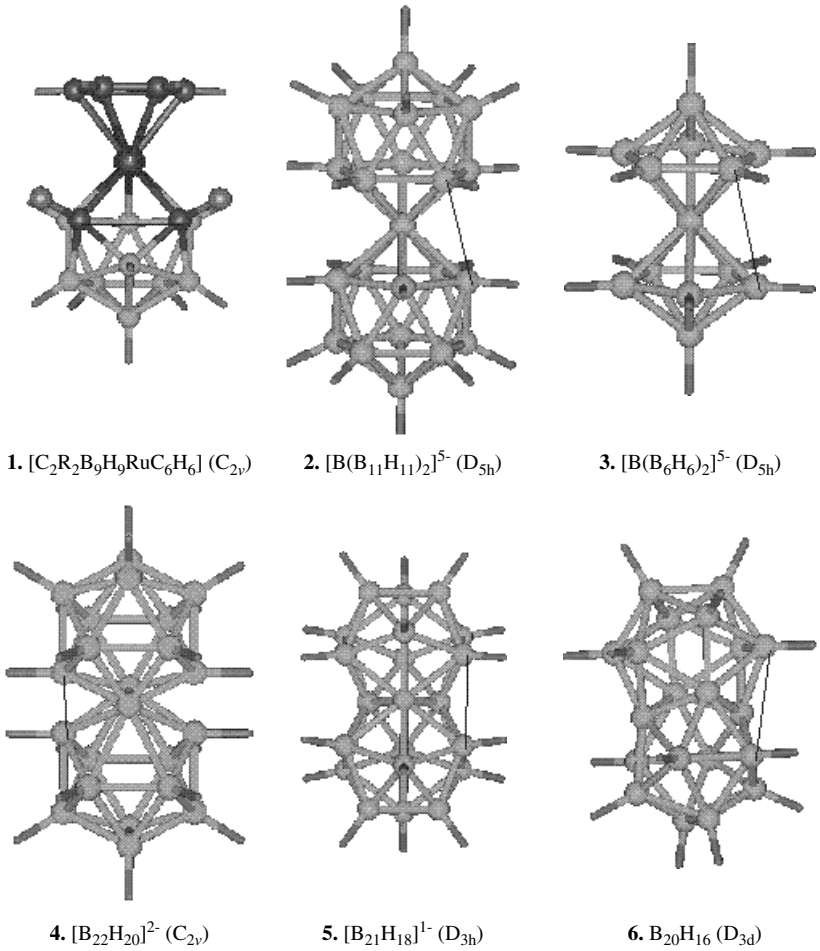

1. $[C_2R_2B_9H_9RuC_6H_6]$ (C_{2v}) **2.** $[B(B_{11}H_{11})_2]^{5-}$ (D_{5h}) **3.** $[B(B_6H_6)_2]^{5-}$ (D_{5h})

4. $[B_{22}H_{20}]^{2-}$ (C_{2v}) **5.** $[B_{21}H_{18}]^{1-}$ (D_{3h}) **6.** $B_{20}H_{16}$ (D_{3d})

Figure 1. All the fusion modes starting from single vertex to four-atom sharing are shown taking a B_{12} unit: $[B(B_{11}H_{11})_2]^{5-}$ (**2**), $[B_{22}H_{20}]^{2-}$ (**4**), $[B_{21}H_{18}]^{-}$ (**5**) and $B_{20}H_{16}$ (**6**). The cap–cap interactions due to condensation are depicted as dotted lines. $[C_2R_2B_9H_9RuC_6H_6]$ (**1**) corresponds to the monopolyhedral system, where such interactions are induced between the vertices of the B_{12} cage. $[B(B_6H_6)_2]^{5-}$ (**3**) corresponds to a sandwich system based on pentagonal bipyramidal skeleton. Structures **2**, **3** and **4** are hypothetical examples. **5** and **6** correspond to the minimized geometries on the PES. **6** is also known experimentally.

makes the molecule a two-cluster system fused through a transition-metal vertex. Macropolyhedral boranes formed by the condensation of two or more polyhedral clusters through one or more boron atoms bring additional complexity, as the non-bonding interactions are suspected to influence their stability.[7] The nature of these interactions is the subject of the current study. Though there are many ways of fusing polyhedral boranes, starting with single vertex to four-atom sharing, mixing the various fusions, alleviating the charges of opened cages by adding bridging hydrogen atoms and so on, progress appears to be hindered due to the suspected steric interactions. The existence of pentalene complexes of metals with both *cis* and *trans* orientations[8–11] prompted us to undertake a detailed analysis of such interactions. Taking the same B_{12} skeleton, Fig. 1 shows the various condensations (**2**, **4**–**6**) known in polyhedral borane chemistry. Here, the dotted lines indicate the interactions between atoms from two adjacent subclusters, which are linked to the same shared atoms. For want of a better term, we call these atoms caps and the interactions between them are termed cap–cap interactions (Fig. 1).

Structure **2**, with all boron atoms, does not exist in an isolated form. However, examples are known with more bulky atoms like aluminum, silicon or some transition metals as the central atom.[12–16] Molecular orbital (MO) studies on sandwich compounds involving octahedral aluminum clusters by various groups have shown that the cap–cap distance, and hence their interactions, is a major factor in determining the stability of sandwich complexes.[17,18] We use a similar approach in studying borane clusters based on a pentagonal bipyramid, $[B(B_6H_6)_2]$ (**3**). Structure **4**, where two B_{12} skeletons share an edge, is not realizable due to the very close distance between the caps (1.5 Å with the experimental B–B distances of $B_{12}H_{12}^{2-}$).[19] All the experimentally known structures with edge sharing exhibit either bis*nido* patterns with open faces opposite to each

other[20–22] or the skeleton has been slightly rearranged.[23] Since the major aspects of interactions between the caps will remain similar in a pentagonal bipyramid, we have considered single-vertex-shared pentagonal bipyramids ($[Al(C_2B_4H_6)_2]^-$ (**7**), Fig. 2) for our study; similar structures are known in abundance.[24–31] We have also taken realizable models in edge-shared systems from *closo* ($B_{12}H_{10}^{2-}$ (**8**), $B_{10}H_8^{2-}$ (**9**)), *nido* ($B_{11}H_{13}$ (**10**)), and *bisnido* ($B_{10}H_{14}$ (**11, 12**)) forms where there is the possibility of cap–cap interactions. When the two cap BH groups of *cis*-$B_{10}H_{14}$ are replaced by CH groups, the molecular formula becomes $C_2B_8H_{12}$ and structure **13** results. This molecule is chosen for the study to find out

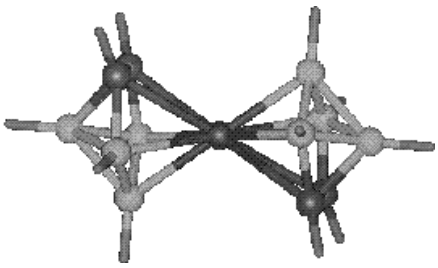

7. $[(C_2B_4H_6)_2Al]^{1-}$ (C_2)

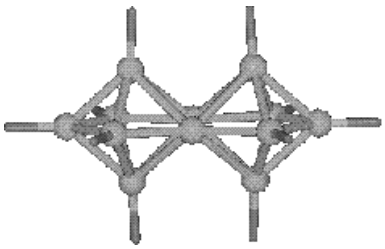

8. $[B_{12}H_{10}]^{2-}$ (D_{2h})

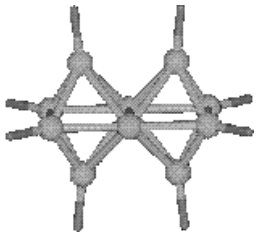

9. $B_{10}H_8^{2-}$ (D_{2h})

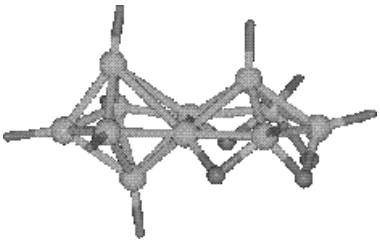

10. $B_{11}H_{13}$ (C_f)

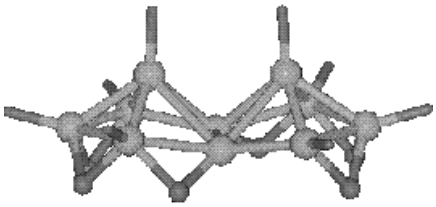

11. *Cis*-$B_{10}H_{14}$ (C_2)

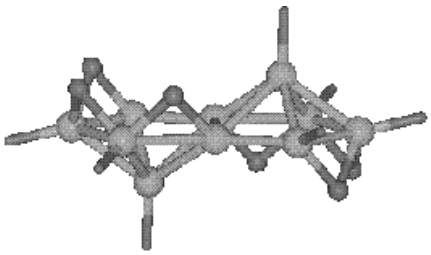

12. *Trans*-$B_{10}H_{14}$ (C_i)

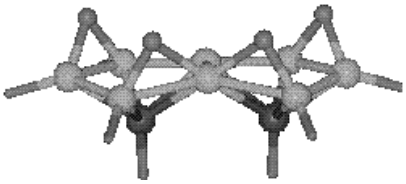

13. $[C_2B_8H_{12}]$ (C_f)

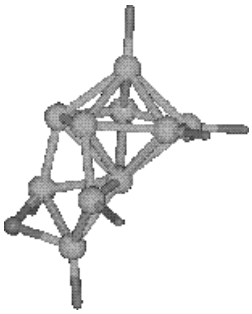

14. $B_{10}H_8^{2-}$ (C_1)

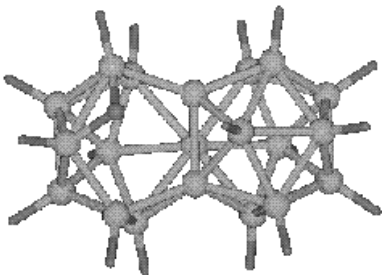

15. $B_{20}H_{18}^{2-}$ (C_1)

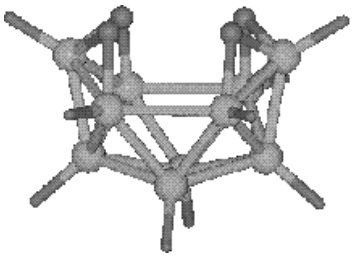

16. $B_{10}H_{14}$ (C_{2v})

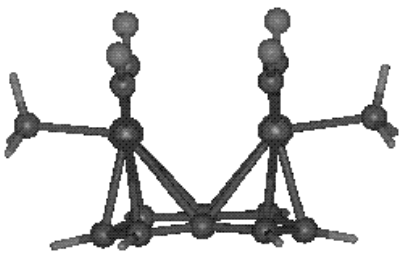

17. *Cis*-$[C_8H_6(Ru(CO)_2Me)_2]$ (C_{2v})

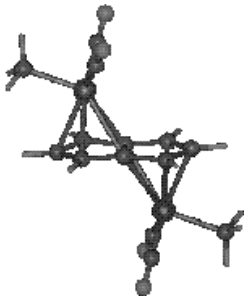

18. *Trans*-$[C_8H_6(Ru(CO)_2Me)_2]$ (C_{2h})

Figure 2. The geometries of the optimized structures used for the study. Structures $[(C_2B_4H_6)_2Al]^-$ (**7**), $[B_{12}H_{10}]^{2-}$ (**8**), $[B_{10}H_8]^{2-}$ (**9** and **14**) $B_{11}H_{13}$ (**10**), *cis*-$B_{10}H_{14}$ (**11**), *trans*-$B_{10}H_{14}$ (**12**), $C_2B_8H_{12}$ (**13**), $[B_{20}H_{18}]^{2-}$ (**15**), $B_{10}H_{14}$ (**16**) are calculated at the B3LYP/6-31g* level and *cis*- and *trans*-$[C_8H_6(Ru(CO)_2Me)_2]$ (**17** and **18**) at the B3LYP/LANL2DZ level. All are minima on the PES.

how the overlap population (OP), which we have taken as an indicator of bonding and antibonding interactions, varies when a different atom other than boron becomes a cap. A comparison across two fusions is possible through **9**, which has a *nido* face-shared isomer (**14**). The *closo* form of the face condensation product of two B_{12} skeletons, $B_{21}H_{18}^-$ (**5**), discussed earlier and which has been the subject of many theoretical studies,[32] is yet to be isolated. We have considered **5**, along with its *nido* form, $B_{20}H_{18}^{2-}$ (**15**),[33,34] in our studies. The structure **15** is derived from the known $B_{20}H_{16}(NCMe)_2$ by the replacement of $NCMe_2$ groups by H^-.[7] After the experimental isolation and structural characterization of this molecule by Lipscomb and coworkers,[7] the existence of the *closo*-$B_{21}H_{18}^-$ (**5**) was predicted. According to Lipscomb and coworkers,[7] the steric interactions between atoms on adjacent clusters in **5** will be larger in relation to those in **6**; the non-bonded distance is less than the sum of the van der Waal's radii. The only known *closo* form among condensed clusters—$B_{20}H_{16}$ (**6**), involving four-atom fusion—was isolated in the early 1960s.[35,36] In this paper, we study the extent of steric interactions that occur in the different condensation modes and how this affects the stability of these molecules.

Another hindrance towards the merging of metallocenes and polyhedral metallaboranes was the absence of an electron counting rule that could be applied to both these structural varieties. We have recently introduced an electron counting rule that could be used for any combination of these structural fragments. All the molecules under study follow this generalized *mno* rule, which predicts the number of skeletal electron pairs for stability as $m+n+o$ (m is the number of cages involved in condensation, n is the number of vertices and o is the total number of single vertex condensations).[37,38] Most of the molecules that have an $m+n$ number of skeletal electron pairs are inclined to show the same trend in the nature of OP. We have taken isomers of $B_{10}H_{14}$ as representative examples for our detailed MO study. This also enables us to compare several classes of isomers ranging from a condensed system with either the presence or absence of the cap–cap interactions (*cis*- and *trans-bisnido*, **11** and **12**) and the known monopolyhedral system (**16**).[39,40] Such a system (**11** and **12**) can be reduced from the experimentally isolated pentalene complexes of metals by isolobal replacement. Whereas *cis*-$B_{10}H_{14}$ has its equivalent in $[C_8H_6(Ru(CO)_2GeMe_3)_2]$ and $[C_8H_6(Re(CO)_3)_2]$, the *trans* form has many isolobal organometallic molecules, one of which is $[Ni(C_3H_5)_2(C_8H_6)]$.[8–11] Thus, we have also considered the *cis* and *trans* forms of $[C_8H_6(Ru(CO)_2Me)_2]$ (**17, 18**). The large $GeMe_3$ group is replaced by Me for computational ease. The single vertex sandwiches, which have $m+n+o$ skeletal electron pairs, have a greater tendency towards antibonding interactions between the caps, depending on the nature and size of the central atom.

COMPUTATIONAL DETAILS

All the borane structures (**5**–**16**), as well as the transition-metal–pentalene complexes (**17**, **18**) discussed above, have been optimized using hybrid Hartree Fock–density functional theory (HF-DFT) and are found to be minima on the potential energy surface (PES). The 6-31g* basis set at the B3LYP level[41–44] (Becke's three-parameter hybrid method with LYP correlation functional) has been employed for boranes and the LANL2DZ basis set with the effective core potentials (ECPs) of Hay and Wadt[45–47] has been used for transition metal complexes, and the calculations have been done using the Gaussian 94 package.[48] We have also carried out DFT calculations using double zeta functional without polarization (DZ) and triple zeta functional with polarization (TZP) on the transition metal complexes at the Becke–Perdew level using Amsterdam density functional (ADF) package, version 2002.03.[49–55] To study the nature of the cap–cap interactions, we have relied on Mulliken OP[56] at both *ab initio* and extended Hückel (EH)[57,58] levels on the *ab initio* optimized geometries of selected structures. The OP is a rough and ready indicator of bonding and antibonding interactions, especially useful when comparisons involve analogous bonding situations.[59,60] Hence, we restrict its use in similar contexts and expect the conclusions on cap–cap interactions to be qualitatively correct. We have also computed the Wiberg bond index (WBI)[61–63] between the caps in the *cis* arrangements as a further verification of the quantitative results obtained. The values of the OP at both *ab initio* and EH levels, the WBI, total energies and the non-bonding B–B distance, and the dihedral angles wherever possible, along the shared atoms are given in Table 1. The relative energies of the isomers, whenever applicable, are given in Table 1. The EH studies have also been used in understanding the bonding and energetics of MOs of some selected systems, which are minima on the PES.

RESULTS AND DISCUSSION

Sandwich complexes involving five-membered rings

Thusfar, sandwich complexes with all boron atoms are not known experimentally, except as a part of β-rhombohedral boron.[64] Let us consider the hypothetical *closo*-$[B(B_6H_6)_2]^{5-}$ (**3**) with the charge of 5− from the *mno* rule. With boron as the sandwiched atom, the two B_5H_5 rings are too close to each other and the OP between the caps is −0.138 (cap–cap distance of 2.577 Å at B–B bonding distance of 1.786 Å). The nature of the cap–cap interaction in **3** is maintained even at a B–B distance found in the experimentally isolated sandwich complexes with heavy atom at the shared site (−0.07 at cap–cap distance of 3.143 Å).

A well characterized structure is available where four boron atoms in the ring are replaced by carbon and the sandwiched boron atom by a larger aluminum atom. The optimized geometry of this structure, $[Al(C_2B_4H_6)_2]^-$ (**7**;

Table 1. The total energies (TEs) of **5**–**16** (B3LYP/6-31g*) and **17**, **18** (B3LYP/LANL2DZ), OPs between the caps calculated using wave functions obtained at the *ab initio* and EH MO levels and the WBI at the *ab initio* level of all molecules, corresponding cap–cap distances *D* and the dihedral angles *A* between the caps along the shared atoms. The relative energies (REs) when isomers are present are given in roman numerals within brackets representing each species with a given molecular formula

Molecule	TE (au)	RE (kcal mol^{-1})	WBI	OP		*D* (Å)	*A* (°)
				Ab initio	EH		
$B_{21}H_{18}^{1-}$ (**5**)	−533.120 37		0.101	0.0514	0.063	2.33	88.3
$B_{20}H_{16}$ (**6**)	−506.908 51		0.043	0.0258	−0.001	2.68	113.7
$[Al(C_2B_4H_6)_2]^{1-}$ (**7**)	−601.057 42		0.001	−0.0068	−0.012	3.72	
$B_{12}H_{10}^{2-}$ (**8**)	−304.283 65		0.097	0.0397	0.053	2.54	95.3
$B_{10}H_8^{2-}$ (**9**)	−253.287 09	0.0 (I)	0.250	0.1112	0.213	2.11	67.4
$B_{11}H_{13}$ (**10**)	−281.179 48		0.024	0.0226	−0.002	2.84	63.7
cis-$B_{10}H_{14}$ (**11**)	−256.892 79	66.9 (II)	0.077	0.0596	0.042	2.49	90.8
trans- $B_{10}H_{14}$ (**12**)	−256.950 59	30.7 (II)					
$C_2B_8H_{12}$ (**13**)	−282.111 41		0.029	−0.0104	−0.041	2.55	63.6
$B_{10}H_8^{2-}$ (**14**)	−253.228 51	36.8 (I)	0.233	0.1445	0.152	2.21	93.0
			0.116	0.0777	0.049	2.38	102.6
$B_{20}H_{18}^{2-}$ (**15**)	−508.193 33		0.063	0.0492	0.038	2.43	94.6
			0.060	0.0485	0.039	2.44	92.4
$B_{10}H_{14}$ (**16**)	−256.999 45	0.0 (II)					
cis-$[C_8H_6(Ru(CO)_2Me)_2]$ (**17**)	−1029.316 59	0.0 (III)	0.058	−0.1592	0.048	3.27	77.0
trans-$[C_8H_6(Ru(CO)_2Me)_2]$ (**18**)	−1029.314 20	1.5 (III)					

Fig. 2), is close to that of the experimental geometry. The non-bonded B–B distances are much larger (3.65 Å) but the OP is negative, though small in magnitude (Table 1). The MOs contributing to this antibonding interaction between the caps are shown in Fig. 3. For the hypothetical structure obtained from **3** by removing four electrons, $[B(B_6H_6)_2]^-$, where the degenerate pairs of MOs are vacant, the non-bonded interactions become favorable (0.035 and 0.007 at cap–cap distances of 2.577 Å and 3.143 Å respectively). A sandwich structure involving Si_3H_3 rings and a central boron atom, $[(Si_3H_3)_2B]^+$, has been characterized as being a minimum on the PES. This follows the *mno* rule if the tetrahedron is treated as a closed polyhedron.[65]

Macropolyhedral boranes involving higher fusions

The edge-shared *closo* structures we have considered are $B_{12}H_{10}^{2-}$ (**8**) and $B_{10}H_8^{2-}$ (**9**). The OPs between the caps of the optimized structures of **8** and **9** are positive at both the *ab initio* and EH levels. The *nido* (**10**), as well as the *cis bisnido* (**11**), form derived from $B_{12}H_{10}^{2-}$ has weak bonding interactions between the caps (Table 1). The OP of −0.002 for $B_{11}H_{13}$ at the EH level is small. Though *cis*- (**11**) and *trans*-$B_{10}H_{14}$ (**12**) can exist in many isomeric forms, depending on the positions of the bridging hydrogen atoms, **11** and **12** are found to be the most stable ones and are discussed here. A comparison of the relative energies of **11** and **12** with their monopolyhedral isomer (**16**) shows that **16** is the most stable form. The *trans* (**12**) and the *cis* (**11**) isomers of $B_{10}H_{14}$ are higher in energy than the monopolyhedron

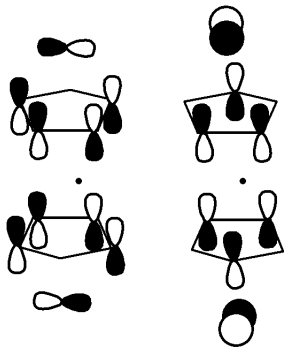

Figure 3. The MOs responsible for the antibonding interactions between the caps in a sandwiched complex with a bridging main group atom. The two MOs will be degenerate in an all-boron sandwich compound.

(**16**) by 30.7 kcal mol^{-1} and 66.9 kcal mol^{-1} respectively. The relative energy shows that the condensation reduces the stability, probably due to the involvement of a larger number of boron atoms at the open area and a lesser number of bridging hydrogen atoms to be placed on the open face of the monopolyhedron compared with **11** or **12**. Structure **16** also has the advantage of being a fragment of an inherently stable icosahedron, whereas **11** and **12** are derived from pentagonal bipyramids. The trend in the calculated energies, at first sight, appears to favor Lipscomb and coworkers' suggestion about the role of cap–cap interactions in the stability of condensed systems.[7]

The next isomers we have considered are of $B_{10}H_8^{2-}$, which exist in a *closo* edge-shared form (**9**) and a *nido* face-shared form (**14**). The cap–cap OPs of these two systems indicate bonding (Table 1). A symmetric form of **14** with an *endo*-hydrogen falls back to the C_1 structure, i.e. **14** with hydrogen bridging two non-shared boron atoms. Another starting structure where the hydrogen bridges a shared and a non-shared atom (**19a**, Fig. 4) converge to a totally different isomer, which is more like an edge-shared system (**19b**, Fig. 4). The energetics show that **14** is less stable than the *closo* edge-shared system **9** by 36.8 kcal mol^{-1}, despite the closer cap–cap distance in **9** (Table 1). Structure **19b** is found to be less stable than **9** by 19.1 kcal mol^{-1}. Thus, short non-bonded distances are not a decisive factor in destabilizing a system.[7] We explain the trend in relative energies of condensed boranes using $B_{10}H_{14}$ isomers as a model in the next section. Condensed boranes involving three- or four-atom fusion show similar trends in the nature of OP. An exception is $C_2B_8H_{12}$ (**13**), which is also studied in detail.

An MO theoretical explanation for cap–cap bonding

The bonding between the caps is studied using the hypothetical $B_{10}H_{14}$ molecule, a model edge-shared system. The *cis* and *trans* isomers of $B_{10}H_{14}$ (**11** and **12**) are analyzed by a ring–cap fragmentation, emphasizing the differences in the two isomers. We restrict our discussion to those MOs involving combinations of the ring π MOs and various combinations of the cap FMOs.[66–68] The special case of $C_2B_8H_{12}$ (**13**) is also analyzed later by comparing the fragment MO (FMO) interactions with $B_{10}H_{14}$. A comparison has also been done with the ruthenium–pentalene complex, which can be fragmented in a similar fashion.

Figure 5 shows an interaction diagram between the ring FMOs ($B_8H_6^{10-}$, center) and the cap FMOs ($(BH^{2+})_2$; left: *trans*, right: *cis*) to give $B_{10}H_8^{6-}$. The skeletons are derived from *closo*-$B_{12}H_{10}^{2-}$ (**8**) and have point group symmetries of C_{2h} and C_{2v} for *trans* and *cis* respectively. From the diagram it is clear that, in the *cis* isomer, there is no occupied MO that has an antibonding interaction between the caps resulting from an end-on-overlap between them. On the other hand, there are occupied MOs with bonding interactions between the caps explaining the positive OP between the caps. The cap OP value for *cis*-$B_{10}H_8^{6-}$ with C_{2v} symmetry is 0.036, which is less than that in *closo*-$B_{12}H_{10}^{2-}$ (0.053). The bending of the five-membered rings in the optimized form of *cis*-$B_{10}H_{14}$ increases the cap–cap overlap to 0.042. The cap–cap OP in $B_{10}H_{14}$ is greater than that in $B_{12}H_{10}^{2-}$, though the WBI between caps is smaller for $B_{10}H_{14}$ according to the *ab initio* results (Table 1).

The *trans* form of $B_{10}H_{14}$ is found to be more stable than the *cis* form by 36.3 kcal mol^{-1}. In the absence of the cap–cap interaction as a factor in explaining the stability between the two isomers, the MOs are analyzed in detail to describe their relative stability. Figure 5 gives a comparison of the stabilization of the ring FMOs due to capping on the same sides or either side of the two five-membered rings fused through an edge. The energies of additional ring FMOs are depicted in Fig. 5. These are FMOs involving in-plane orbitals of the ring boron atoms, which influence the energetics of the MOs we are concerned with, by second-order interactions. The stabilization energies of the ring FMO due to the cap are given in brackets at appropriate places.

Although there are many interactions of varying importance shown in Fig. 5, we concentrate on the strongest among these. These involve the b_{3g}, $2b_{1u}$ and a_u FMOs of the ring. The ring FMO b_{3g} finds its equivalent cap FMO with matching symmetry in b_g of the *trans* arrangement and in b_2 of the *cis* arrangement. b_g (Fig. 5, left) corresponds to an antibonding cap FMO, whereas b_2 (Fig. 5, right) is a bonding cap FMO. The in-plane ring FMOs that can interact with these cap FMOs will be different in *cis* and *trans* forms. Thus, whereas in the *trans* form the b_{3g} is more stabilized due to a second-order interaction from b_{1g}, in the *cis* form the b_{3g} stabilization due to caps is reduced by the second-order interaction from b_{2u}. In a similar way, the next ring FMO, $2b_{1u}$, has a second-order interaction in both *trans* and *cis* forms, with *trans* being affected by b_{3u} and *cis* by the nearer $2a_g$. With the two levels

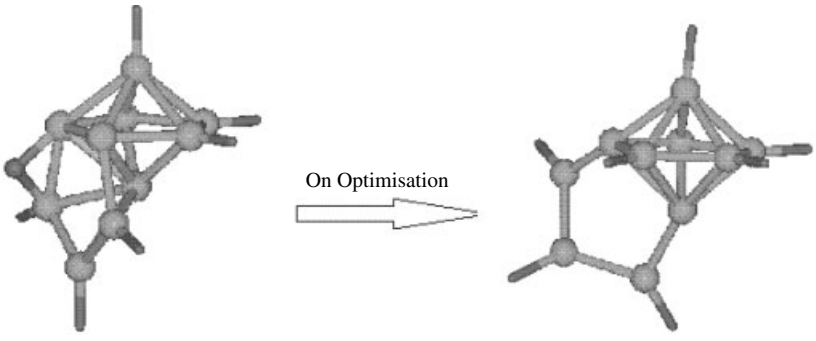

19a. $B_{10}H_8^{2-}$ **19b**. $B_{10}H_8^{2-}$

Figure 4. The structure of *nido* face-shared $B_{10}H_8^{2-}$ (**19a**, left) with the bridging hydrogen between a shared and a non-shared atom converges to structure **19b** on the right-hand side on optimization. **19b** corresponds to the geometry at the B3LYP/6-31g* level of theory.

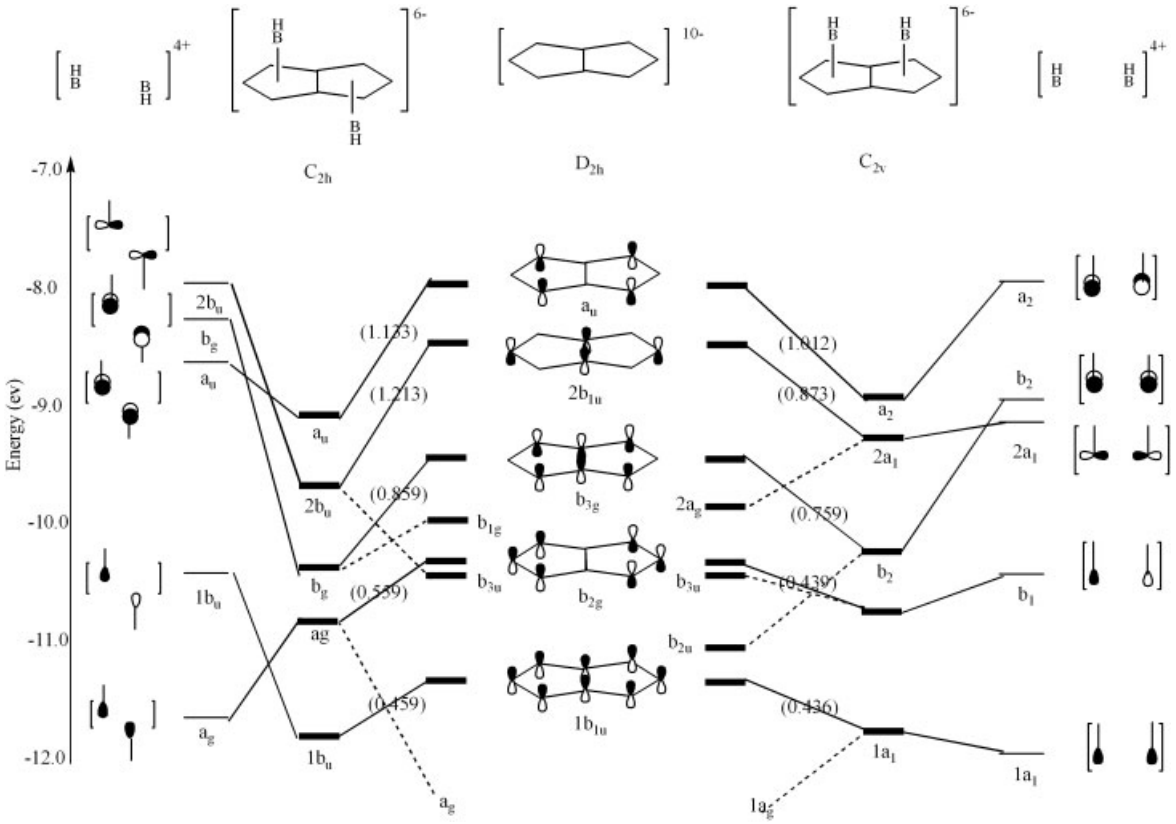

Figure 5. The MOs of *cis*- and *trans*-$B_{10}H_{14}$ (right and left respectively) obtained by an interaction between an edge-shared B_8 ring and two BH groups. Only the MOs involving p orbitals perpendicular to the ring are considered. The magnitude of stabilization of the ring FMOs due to the caps is given in brackets in electronvolts. The dotted lines correspond to secondary interactions.

being farther apart in *trans* than in *cis*, the destabilization is less in *trans* than in *cis*. The highest level, a_u, of the ring has a lesser stabilization due to caps in *cis* than in *trans* despite the closer interacting levels in *cis* than in *trans*. The symmetry-matching cap FMO a_2 in the *cis* form for the ring FMO a_u has antibonding character between the caps, which explains the lesser stabilization in *cis* than in *trans*. The analysis shows the lower stability of *cis* over *trans* as being due to the lesser stabilization of the ring on capping caused by the resulting second-order interactions from lower lying levels competing for the same cap FMO. In general, it is observed that destabilizing second-order interactions are prominent in the *cis* form, which reduces its stability over the *trans* form.

An EH analysis on *cis*-$B_{10}H_8^{6-}$, correlating the initial C_{2v} and the final C_2 geometries (Fig. 6), shows a decrease in the total one-electron energies of the skeleton, with C_2 being the optimized geometry of *cis*-$B_{10}H_{14}$. The *trans* form has a net destabilization when the one-electron energies are correlated between the C_{2h} and the optimized C_i geometries (Fig. 6), though the trend in relative energies between *cis* and *trans* form remains the same. The two five-membered rings deviate from planarity and subtend an angle of 159.0° instead of 180°. One of us had shown earlier that the out-of-plane bending of substituents in a ring increases its overlap with the cap.[66–68] Here, both the caps benefit from the non-planarity of the two rings. As a consequence, the cap–cap distance decreases. There is also a contribution from the cap–cap bonding interaction towards the final geometry. The MOs that are greatly affected in the *cis* form are $2a_1$ and a_2 (Fig. 6), with stabilization energies of 0.485 eV and 0.283 eV respectively. In $2a_1$ the bonding between the caps helps in a greater stabilization of the MO compared with a_2, which has antibonding nature between the caps. Thus, the bending of the ring can be partly attributed to the enhancement of cap–cap overlap in addition to the increase in ring–cap overlap.[66–68] This is also reflected in the shortened cap–cap distance in *cis*-$B_{10}H_{14}$ (**11**) compared with that of the *closo*-$B_{12}H_{10}^{2-}$ (**8**) (2.491 Å versus 2.537 Å; Table 1).[33,34]

In **13**, where the caps are CH groups, the OP is found to be negative (Table 1). This suggests that the MOs responsible for the negative OP in **13** correspond to the in-plane FMOs of the ring, rather than the perpendicular set that is common for all higher fusions. Among the various isomers possible for $C_2B_8H_{12}$, which depend on the position of bridging hydrogen atoms, **13** is the most stable one where the *cis* arrangement is retained, with the others converging to a skeleton where one of the carbon atoms occupies a lesser coordination site. A comparative analysis between the interaction diagrams for

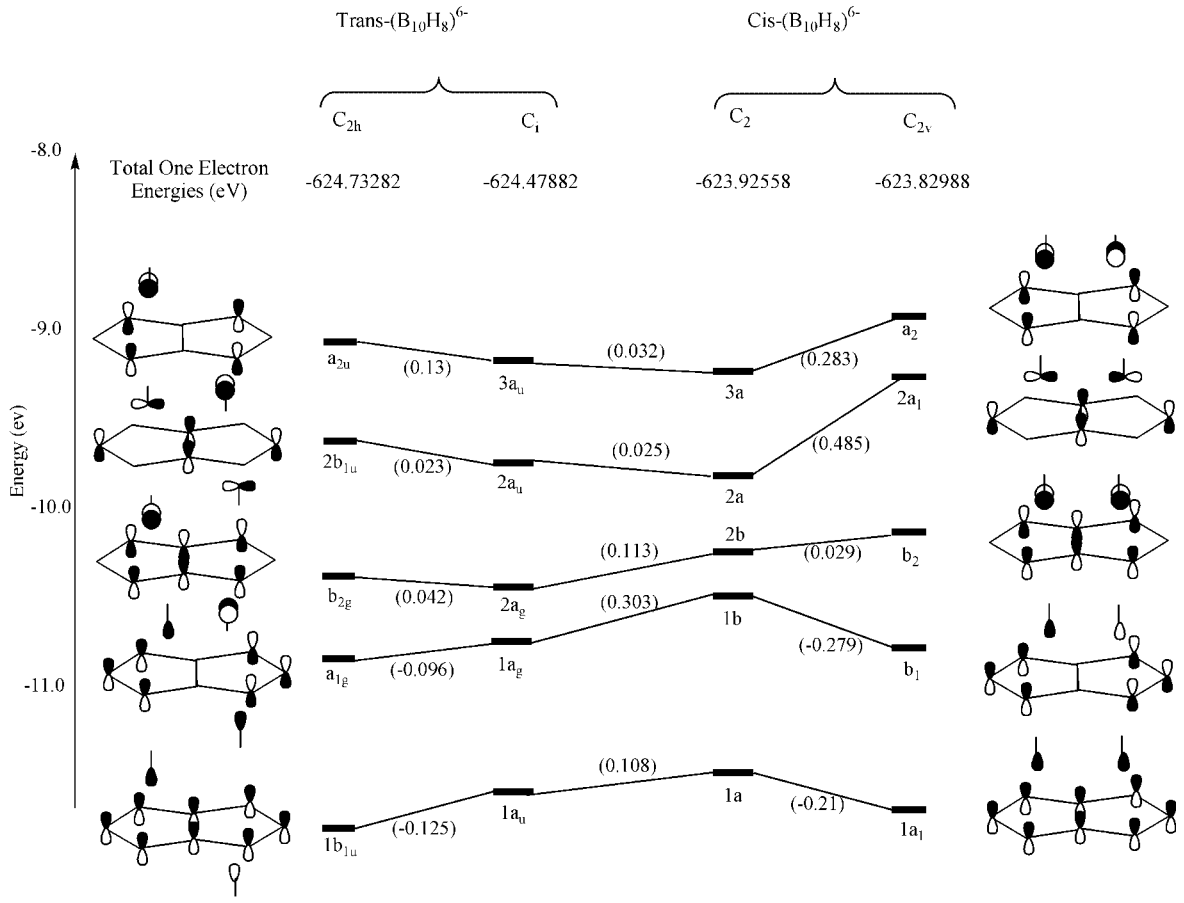

Figure 6. A correlation diagram between the C_{2h} and C_i geometries of *trans*-$B_{10}H_8^{6-}$ (left) and between C_{2v} and C_2 geometries of *cis*-$B_{10}H_8^{6-}$ (right) is given. Only the MOs involving p orbitals perpendicular to the ring are shown.

CH and BH caps shows that the difference lies in an MO with contribution from an in-plane ring FMO. The interaction that results in this MO is shown in Fig. 7, which clearly illustrates the higher contribution of the antibonding cap FMO when CH becomes the caps. The reason is obviously the greater electronegative nature of carbon, which brings down the energy levels. Thus the cap FMO shown in Fig. 7, which is responsible for the antibonding nature between the caps, is very close to the ring FMO and has a strong interaction, resulting in the greater stabilization of the ring FMO. This is clear from the percentage contribution of the cap FMOs to this particular MO in the two compounds. Whereas in $B_{10}H_8^{6-}$ there is only 12% contribution, $C_2B_8H_8^{4-}$ has 43% contribution from the cap FMO to the resultant MO shown in Fig. 7.

Analogy of macropolyhedral boranes with organometallic pentalene complexes

We have attempted a comparison between $B_{10}H_{14}$ and its isolobal analog, the pentalene–ruthenium complex, which is known in its *cis* form (**17**).[8,10] The experimental report on the *cis* form suggests the presence of a bond between the two ruthenium atoms at a distance of 3.0 Å. A bond between the metals is presumed based on the 18-electron rule (Ru^{2+} has six electrons, two CO groups donate four electrons, Me^- has two, and $C_8H_6^{2-}$ donates $10/2 = 5$, leading to the 17 electrons count); the M–M σ bond completes the 18 electrons. The *trans* orientation of **17** is also predicted on the basis of reported geometries of isoelectronic molecules like *trans*-$[Ni(C_3H_5)_2(C_8H_6)]$. The *trans* arrangement is explained as a structure resonating between two forms with one of the metals having 16 and the other 18 electrons around it.[9] The understanding of the bonding in these systems can be simplified by the application of the *mno* rule where one considers the entire cluster to be delocalized.[37,38] Thus, according to the *mno* rule, $m = 2$, $n = 10$, $o = 0$ and there are two *nido* faces, which predicts a total of 14 $(2 + 10 + 2)$ skeletal electron pairs for stability. This is achieved from six CH (nine electron pairs), two carbon atoms (four) and two d^7 ML_3 fragments isolobal to BH^+ (one). Thus, the cluster electron count remains the same for the *cis* and *trans* structures. The metal, as well as the cluster, attains its stable electron count without invoking resonance in the *trans* structure alone. Thus, the *mno* rule is more preferred for complexes with condensed ligands.

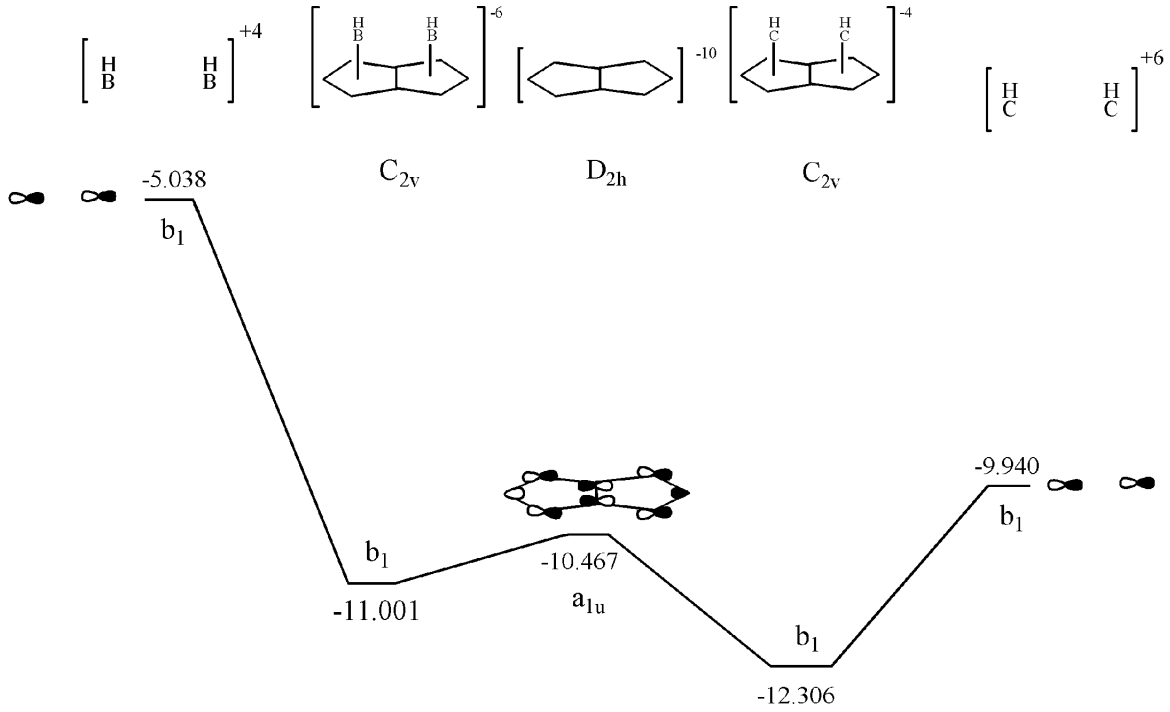

Figure 7. Comparison of the interaction when two BH (left) and two CH (right) cap the B_8 ring in the *cis* form, leading to b_1. The cap FMO (b_1, right) is very close to the ring FMO (a_u) when CH is used as caps. The higher contribution of the CH cap FMO results in an antibonding interaction between the caps.

On optimization of $[C_8H_6(Ru(CO)_2Me)_2]$ at *cis* (**17**) and *trans* (**18**) orientations, we found that the *cis* form is more stable than the *trans* form by 1.5 kcal mol^{-1} at the B3LYP/LANL2DZ level and by 1.3 kcal mol^{-1} at Becke–Perdew level using DZ basis set. The optimized structure of **17** has somewhat longer metal–metal distances of 3.270 Å and 3.20 Å at B3LYP/LANL2DZ and BP86/DZ levels respectively. Inclusion of polarization functions, (a triple zeta basis (BP86/TZP)), changes the M–M bond distance marginally to 3.21 Å. Some of the important structural parameters of **17** at the experimental geometry and at various levels of theory are given in Table 2 for comparison. The dihedral angle C_m–C_s–C_s–C_m (Table 2) in **17** is the angle subtended by the two planar five-membered rings and is bent away from the caps. Although the calculated value at all three levels is around 174°, the experimental structure has an average value of 176.6° (values varying from 173° to 178°). The bending of the ring away from the caps, in contrast to that observed in *cis*-$B_{10}H_{14}$ (**11**), is due to the more diffuse metal orbitals with a smaller carbon ring.[66–68] The OPs between the metals in the experimental and the LANL2DZ optimized geometries are found to be positive at the EH level with values of 0.041 and 0.048 respectively; but a higher *ab initio* level shows an antibonding interaction with an OP of −0.1592. The repulsive nature between the metals identified at higher levels of theory is an added reason for bending of the five-membered rings in pentalene compared with that observed in the experimental geometry. This helps in increasing the M–M distance, thereby overcoming the possible repulsion between them. Natural bond order studies[61–63] on the optimized geometry suggest that there is no bond between the two metals. Further, the near-equal stability of the *trans* form leads us to conclude that there is practically no bonding interaction between the two metals in the *cis* form.

An FMO analysis is done on the optimized geometries of both *cis* and *trans* forms by following a similar fragmentation of rings and caps. Similar EH studies have been done for sandwich complexes of pentalene, $[M_2(C_8H_6)_2]$ (M = Co, Ni), where the OP between metals is found to be zero.[69,70] The important interactions in the *cis* and *trans* forms (**17** and **18**) that lead to the stabilization of the ring FMOs are shown in Figs 8 and 9 respectively. The Mulliken symbols assigned to the orbitals are based on the symmetry of the resultant molecule and assuming a similar coordinate system in the fragments. The d^7L_3M–d^7ML_3 bimetallic part with three ligands arranged in a conical manner on each metal has its octahedral remnants, the bonding and antibonding contributions of the t_{2g} sets, i.e. $(t_{2g} + t_{2g})$ and $(t_{2g} - t_{2g})$, occupied. The remaining two electrons will occupy the most bonding FMO (a_1, Fig. 8) between the metals. In Fig. 8, a_1 is shown to be empty, as the binuclear metal fragment is considered to be dicationic, donating the two electrons to the C_8H_6 ligand. The $2b_2$ and a_2 orbitals of the *cis* structure stabilize the ring FMOs (Fig. 8). The $(t_{2g} - t_{2g})$ remains almost non-bonding here, whereas the $(t_{2g} + t_{2g})$ participates in two-orbital–four-electron interactions. One

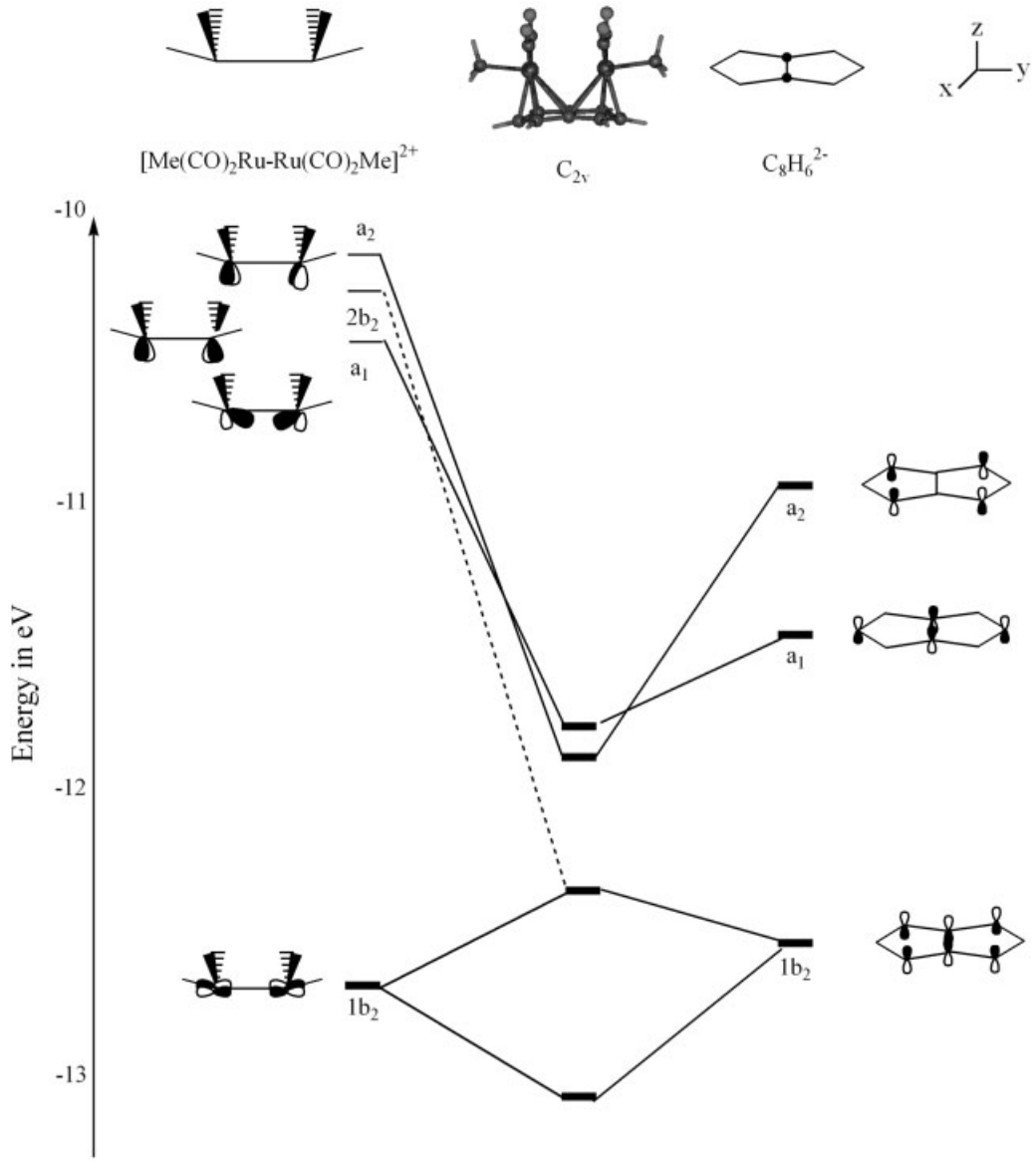

Figure 8. The interaction diagram between the ring and caps of the *cis* isomer of $[C_8H_6(Ru(CO)_2Me)_2]$. All the stabilizing interactions and one representative two-orbital–four-electron interaction are shown. Here, $(t_{2g} - t_{2g})$ remains almost non-bonding and $(t_{2g} + t_{2g})$ is involved in two-orbital–four-electron interactions. The geometry of *cis*-$[C_8H_6(Ru(CO)_2Me)_2]$ corresponds to the optimized one at B3LYP/LANL2DZ.

such combination is depicted in Fig. 8, where two $1b_2$ fragments interact. Here, the antibonding combination is stabilized by the high-lying $2b_2$ level on the metal side. The highest occupied MO (HOMO; a_1) of the molecule has a bonding interaction between the metals. Removal of two electrons from this MO results in zero OP between the metals by EH studies. In the *trans* form (**18**), the stabilizing interactions are decreased (Fig. 9). Here, the $(t_{2g} + t_{2g})$ set remains almost non-bonding, whereas the $(t_{2g} - t_{2g})$ is involved in two-orbital–four-electron interactions. The HOMO of **18** is one such antibonding level resulting from the interaction between two $1b_u$ orbitals. The HOMO is stabilized by a higher lying $2b_u$ FMO on the metal fragment. Only one level (a_u) is involved in a two-orbital–two-electron interaction. Though the second-order stabilizing interactions are present even in the *trans* structure, their magnitude is less because interactions come from MOs with antibonding character between the metals and are high in energy.

CONCLUSIONS

The common belief that the interactions between two non-bonded proximate atoms are repulsive in polycondensed

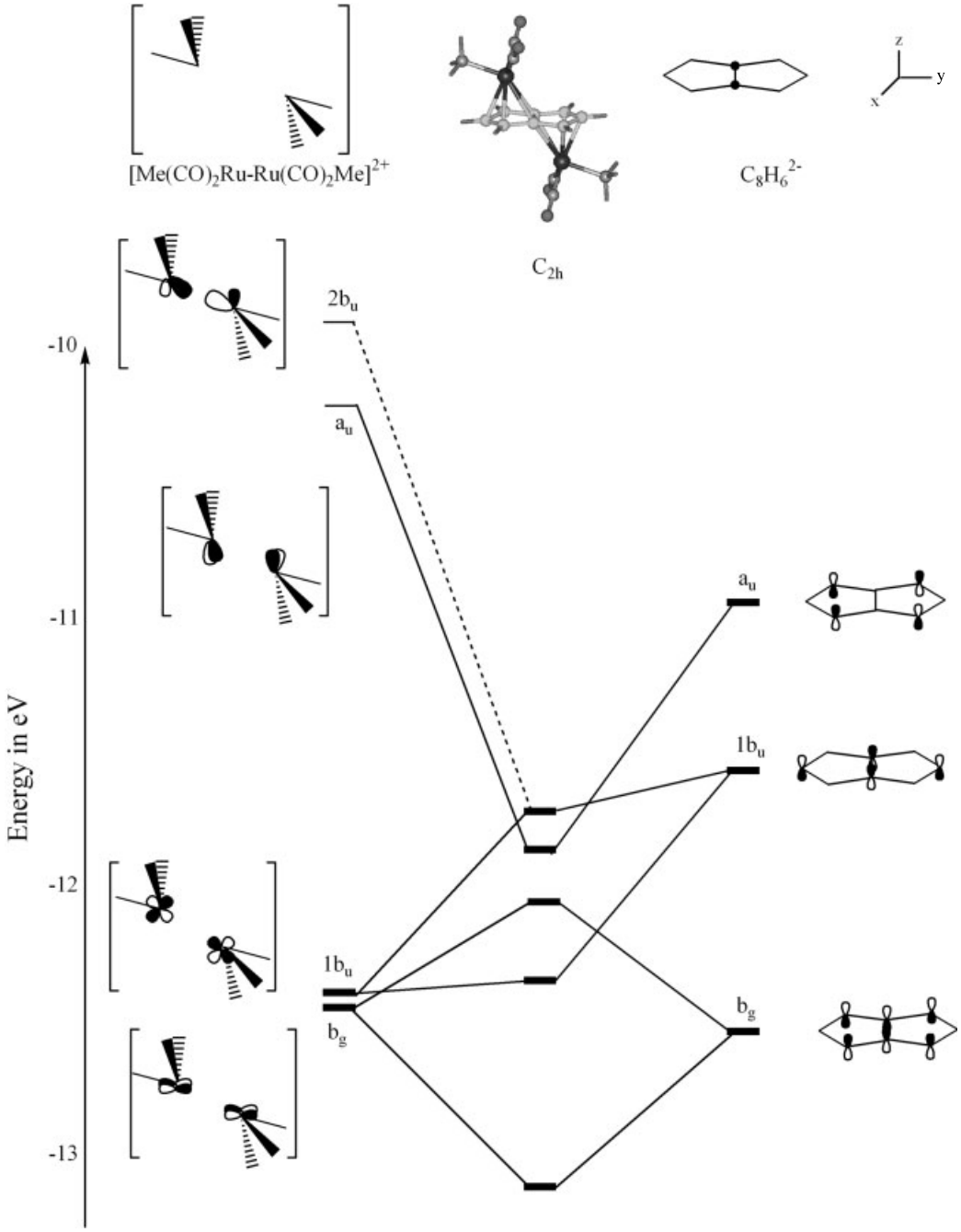

Figure 9. The interaction diagram showing the formation of the *trans* isomer of $[C_8H_6(Ru(CO)_2Me)_2]$ from the ring and caps. All the stabilizing interactions and one representative of the two-orbital–four-electron interaction are shown. Here, $(t_{2g} + t_{2g})$ remains almost non-bonding and $(t_{2g} - t_{2g})$ is involved in two-orbital–four-electron interactions. The geometry of *trans*-$[C_8H_6(Ru(CO)_2Me)_2]$ corresponds to the optimized one at B3LYP/LANL2DZ.

boranes is not found to be generally true. We have analyzed the problem using model systems from two areas: polyhedral borane chemistry and organometallic chemistry. The hypothetical model, $B_{10}H_{14}$, used in condensed boranes is derived from the experimentally isolated $[C_8H_6(Ru(CO)_2GeMe_3)_2]$. This enabled a further analysis among various isomers of $B_{10}H_{14}$. The energy changes involved due to the condensation of open polyhedral boranes has thus been explored using $B_{10}H_{14}$ as the model. The relative stability between the two isomers of $B_{10}H_{14}$ (**11** and **12**) has been explained based on a detailed FMO approach. The difference in the nature of the OP between the caps in sandwich and higher fusions involving boron atoms has been understood by an MO study. The nature of the bonding between the caps is attributed to

Table 2. Some important parameters of *cis*-[$C_8H_6(Ru(CO)_2Me)_2$] at the experimental and theoretical geometries at B3LYP/LANL2DZ, BP86/DZ and BP86/TZP. C_s is the shared carbon. C_m connects C_s and a non-shared carbon. C_t bonds two C_m. RE is the relative energy with its *trans* isomer. The distances and dihedral angles are averaged in the experimental geometry

Parameters	Experimental	B3LYP/ LANL2DZ	BP86/ DZ	BP86/ TZP
Ru–Ru (Å)	3.06	3.27	3.20	3.21
Ru–C_s (Å)	2.52	2.65	2.64	2.61
Ru–C_m (Å)	2.22	2.37	2.37	2.33
Ru–C_t (Å)	2.17	2.27	2.30	2.24
C_s–C_s (Å)	1.43	1.46	1.46	1.45
C_s–C_m (Å)	1.44	1.45	1.45	1.44
C_m–C_t (Å)	1.35	1.45	1.45	1.43
C_m–C_s–C_s–C_m (°)	176.3	174.5	173.5	174.3
RE (kcal mol^{-1})		1.5	1.4	1.8

the absence of cap–cap end on overlap which is antibonding, unlike in sandwich complexes. The additional MO in sandwich compounds has a predominant antibonding character between the caps, which results in a negative OP in these systems. The magnitude of these destabilizing interactions in single-vertex sandwiches depends on the size and nature of the central atom. The results of the study demonstrate the significance of cap–cap interactions in the stability of higher fusions, regardless of the experimental abundance of only *trans* isomers in edge-shared systems. The higher stability of *closo* edge-shared $B_{10}H_8^{2-}$ (**9**) over its *nido* face-shared isomer (**14**) is a further support for this argument. The negative OP in edge-shared dicarbaboranes with two CH as caps (**13**) is due to the greater contribution of the cap–cap antibonding FMO to one of the in-plane ring FMOs. This arises from the greater electronegativity of carbon, which brings down the cap FMO closer to the interacting ring FMO. The positive OP of 0.048 at the EH level between ruthenium atoms in the pentalene complexes reflects weak bonding interactions between them; this becomes slightly antibonding at higher levels. Therefore, it is better to treat the pentalene complex under the *mno* rule rather than the 18 electron rule. The almost equal stability of the *cis* and *trans* forms supports this conclusion. Appropriate macropolyhedral borane equivalents await experimental scrutiny.

Acknowledgements

We thank the Council of Scientific and Industrial Research (CSIR), New Delhi, and the Board of Research in Nuclear Sciences (BRNS), Mumbai, for providing financial support for this work. PDP acknowledges the research fellowship from CSIR. The University with Potential for Excellence (UPE) project of UGC, New Delhi, India, also helped this study.

REFERENCES

1. Casanova J. *The Borane, Carborane, Carbocation Continuum*. John Wiley & Sons: New York, 1998.
2. Hoffmann R. *Angew. Chem. Int. Ed. Engl.* 1982; **21**: 711.
3. Lei X, Shang M, Fehlner TP. *Angew. Chem. Int. Ed. Engl.* 1999; **38**: 1986 and references cited therein.
4. Kennedy JD. Macropolyhedral boron-containing cluster chemistry. Overview and recent developments. In *Advances in Boron Chemistry*, Seibert W (ed.). Royal Society of Chemistry: London, 1997; 451–462.
5. Grimes RN. Metal–carborane sandwiches and macromolecular assemblies. In *Advances in Boron Chemistry*, Seibert W (ed.). Royal Society of Chemistry: London, 1997; 321–332.
6. McWhannell MA, Rosair GM, Welch AJ, Teixidor F, Vinas C. *J. Organometal. Chem.* 1999; **573**: 165.
7. Enemark JH, Friedman LB, Lipscomb WN. *Inorg. Chem.* 1966; **5**: 2165.
8. Brookes A, Howard J, Knox SAR, Stone FGA, Woodward P. *J. Chem. Soc. Chem. Commun.* 1973; 587.
9. Harris PJ, Howard JAK, Knox SAR, McKinney RJ, Philips RP. *J. Chem. Soc. Dalton. Trans.* 1978; 403.
10. Howard JAK, Woodward P. *J. Chem. Soc. Dalton. Trans.* 1978; 412.
11. Jones SC, Hascall T, Barlow S, O'Hare D. *J. Am. Chem. Soc.* 2002; **124**: 11 610.
12. Schubert DM, Bandman MA, Rees WS Jr, Knobler CB, Lu P, Nam W, Hawthorne MF. *Organometallics* 1990; **9**: 2046.
13. Kang HC, Lee SS, Knobler CB, Hawthorne MF. *Inorg. Chem.* 1991; **30**: 2024.
14. Deboer BG, Zalkin A, Templeton DH. *Inorg. Chem.* 1968; **7**: 2288.
15. Warren LF Jr, Hawthorne MF. *J. Am. Chem. Soc.* 1970; **92**: 1157.
16. Rees WS Jr, Schubert DM, Knobler CB, Hawthorne MF. *J. Am. Chem. Soc.* 1986; **108**: 5369.
17. Vajenine GV, Hoffmann R. *J. Am. Chem. Soc.* 1998; **120**: 4200.
18. Jemmis ED, Jayasree EG. *Collect. Czech Chem. Commun.* 2002; **67**: 965.
19. Jemmis ED, Balakrishnarajan MM, Pancharatna PD. *Inorg. Chem.* 2001; **40**: 1730.
20. Pitochelli AR, Hawthorne MF. *J. Am. Chem. Soc.* 1962; **84**: 3218.
21. Simpson PG, Folting K, Dobrott RD, Lipscomb WN. *J. Chem. Phys.* 1963; **39**: 26.
22. Simpson PG, Lipscomb WN. *J. Chem. Phys.* 1963; **39**: 2339.
23. Hosmane NS, Franken A, Zhang G, Srivastava RR, Smith RY, Speilvogel BF. *Main Group Met. Chem.* 1998; **21**: 319.
24. Siriwardane U, Islam MS, West TA, Hosmane NS, Maguire JA, Cowley AH. *J. Am. Chem. Soc.* 1987; **109**: 4600.
25. Hosmane NS, de Meester P, Siriwardane U, Islam MS, Chu SSC. *J. Chem. Soc. Chem. Commun.* 1986; 1421.
26. Hosmane NS, Lu KJ, Zhang H, Maguire JA. *Organometallics* 1997; **16**: 5163.
27. Hosmane NS, de Meester P, Siriwardane U, Islam MS, Chu SSC. *J. Am. Chem. Soc.* 1986; **108**: 6050.
28. Islam MS, Siriwardane U, Hosmane NS, Maguire JA, de Meester P, Chu SSC. *Organometallics* 1987; **6**: 1936.
29. Hosmane NS, Zhu D, McDonald JE, Zhang H, Maguire JA, Gray TG, Helfert SC. *J. Am. Chem. Soc.* 1995; **117**: 12 362.
30. Hosmane NS, Yang J, Zhang H, Maguire JA. *J. Am. Chem. Soc.* 1996; **118**: 5150.
31. Grimes RN. *Metal Interactions with Boron Clusters*. Plenum Press: New York, 1982.
32. Lipscomb WN. *J. Less-Common Met.* 1981; **82**: 1.
33. Jemmis ED, Balakrishnarajan MM, Jayasree EG. In preparation.
34. Jemmis ED, Balakrishnarajan MM, Pancharatna PD. *Chem. Rev.* 2002; **102**: 93.
35. Friedman LB, Dobrott RD, Lipscomb WN. *J. Am. Chem. Soc.* 1963; **85**: 3506.
36. Miller HC, Muetterties EL. *J. Am. Chem. Soc.* 1963; **85**: 3506.

37. Balakrishnarajan MM, Jemmis ED. *J. Am. Chem. Soc.* 2000; **122**: 4516.
38. Jemmis ED, Balakrishnarajan MM, Pancharatna PD. *J. Am. Chem. Soc.* 2000; **123**: 4313.
39. Moore EB Jr, Dickerson RE, Lipscomb WN. *J. Chem. Phys.* 1957; **27**: 209.
40. Brill R, Dietrich H, Dierks H. *Acta Crystallogr. Sect. B* 1971; **27**: 2003.
41. Becke AD. *J. Chem. Phys.* 1993; **98**: 5648.
42. Lee C, Yang W, Parr RG. *Phys. Rev. B* 1988; **37**: 785.
43. Vosko SH, Wilk L, Nusair M. *Can. J. Phys.* 1980; **58**: 1200.
44. Stephens PJ, Delvin FJ, Chabalowski CF, Frisch MJ. *J. Phys. Chem.* 1994; **98**: 11 623.
45. Hay PJ, Wadt WR. *J. Chem. Phys.* 1985; **82**: 270.
46. Wadt WR, Hay PJ. *J. Chem. Phys.* 1985; **82**: 284.
47. Hay PJ, Wadt WR. *J. Chem. Phys.* 1985; **82**: 299.
48. Frisch MJ, Trucks GW, Schelegel HB, Gill PMW, Johnson BG, Robb MA, Cheeseman JR, Keith T, Peterson GA, Montgomery JA, Raghavachari K, Al-Laham MA, Zakrzewski VG, Oritz JV, Foresman JB, Cioslowsky J, Stefenov BB, Nanayakkara A, Callacombe M, Peng CY, Ayala PY, Chen W, Wong MW, Andres JL, Replogle E, Gomberts R, Martin RL, Fox DJ, Binkley JS, Defrees DJ, Baker J, Stewart JP, Head-Gordon M, Gonzalez C, Pople JA. *Gaussian-94*, revision D.I. Gaussian Inc., Pittsburgh, PA, 1995.
49. Baerends EJ, Ellis DE, Ros P. *Chem. Phys.* 1973; **2**: 42.
50. Boerrigter PM, Velde G, Baerends EJ. *Int. J. Quantum Chem.* 1988; **33**: 87.
51. Becke AD. *Phys. Rev. A* 1988; **38**: 2398.
52. Perdew JP. *Phys. Rev. B* 1986; **33**: 8822.
53. TeVelde G, Bickelhaupt FM, van Gisbergen SJA, Guerra CF, Baerends EJ, Snijders JG, Ziegler T. *J. Comput. Chem.* 2001; **22**: 931.
54. Guerra CF, Snijders JG, TeVelde G, Baerends EJ. *Theor. Chem. Acc.* 1998; **99**: 391.
55. ADF2002.03, SCM, Theoretical Chemistry, Vrije Universiteit, Amsterdam, The Netherlands. URL: http://www.scm.com..
56. Mulliken RS. *J. Chem. Phys.* 1955; **23**: 1481.
57. Hoffmann R, Lipscomb WN. *J. Chem. Phys.* 1962; **36**: 2179.
58. Hoffmann R. *J. Chem. Phys.* 1963; **39**: 1397.
59. Albright TA, Burdett JK, Whangbo M-H. *Orbital Interactions in Chemistry*. Wiley–Interscience: New York, 1985.
60. Glassey WV, Hoffmann R. *J. Chem. Phys.* 2000; **113**: 1698.
61. Reed AE, Weistock RB, Weinhold F. *J. Chem. Phys.* 1985; **83**: 735.
62. Reed AE, Curtiss LA, Weinhold F. *Chem. Rev.* 1988; **88**: 899.
63. Weiberg KB. *Tetrahedron* 1968; **24**: 1083.
64. Jemmis ED, Balakrishnarajan MM. *J. Am. Chem. Soc.* 2001; **123**: 4324.
65. Srinavas GN, Hamilton TP, Jemmis ED, McKee ML, Lammertsma K. *J. Am. Chem. Soc.* 2000; **122**: 1725.
66. Jemmis ED, Schleyer PvR. *J. Am. Chem. Soc.* 1982; **104**: 4781.
67. Jemmis ED. *J. Am. Chem. Soc.* 1982; **104**: 7017.
68. Jemmis ED, Pavankumar PNV. *Proc. Ind. Acad. Sci. (Chem. Sci.)* 1984; **93**: 479.
69. Burdett JK, Canadell E. *Organometallics* 1985; **4**: 805.
70. Cloke FGN, Green JC, Jardine CN, Kuchta MC. *Organometallics* 1999; **18**: 1087.